Sikanni Bridge Fire - Triaging an Emergency Response

Matthew Bowser, M.A.Sc., P.Eng.
Senior Project Manager
WSP Canada Inc.
Nanaimo, BC
Matthew.Bowser@wsp.com

Christopher Mantha, M.A.Sc., P.Eng.
Acting Senior Engineer, Bridges and Transportation Structures
Public Service Procurement Canada
Halifax, Nova Scotia
Christopher.Mantha@pwgsc-tpsgc.gc.ca

Sascha Schreiber, M. Sc., P.Eng., ENV SP
Chief Engineer, Bridges and Transportation Structures
Public Services Procurement Canada
Gatineau, Quebec
Sascha.Schreiber@tpsgc-pwgsc.gc.ca

Jianping Jiang, Ph.D., P.Eng.
National Practice Leader, Bridges & Civil Structures
WSP Canada Inc.
Vancouver, BC
Jianping.Jiang@wsp.com

Christopher Morgan, M.Sc., P.Eng.
Manager, Bridges
WSP Canada Inc.
Saskatoon, SK
Christopher.Morgan@wsp.com

Christie Corrigan, EIT
EIT, Bridges
WSP Canada Inc.
Vancouver, BC
Christie.Corrigan@wsp.com

Paper prepared for the session ST - Transportation Structures
2024 Transportation Association of Canada (TAC) Conference & Exhibition
Vancouver, British Columbia

Abstract

In August 2022, a transport tanker carrying a highly flammable liquid crashed into the south approach barriers at the Sikanni Chief River Bridge resulting in a full closure of the Alaska Highway (Highway 97) in northern BC. The fire generated intense heat that resulted in extensive structural damage and brought forward severe concerns for weakening of the bridge load carrying members. As a critical link to Northern Canada and then to Alaska, USA, there was extreme pressure to get this highway safely re-opened as quickly as possible. An emergency response was initiated immediately with a rapid damage assessment that enabled light vehicle traffic to be restored shortly after the incident. The emergency response and structural assessment continued until full unrestricted truck traffic was restored on the bridge. While the primary focus was forensic review and structural evaluation of the residual load carrying capacity, several concurrent bridge engineering teams were mobilized to work in parallel, developing contingency plans that were on hand in case the structural evaluation demonstrated insufficient capacity for truck traffic. Concurrent teams completed forensic review; load testing; structural evaluation for load carrying capacity of the bridge in its damaged state; detour crossing planning; fibre-reinforced polymer strengthening of fire damaged concrete girders; and external strengthening of fire damaged superstructure.

For the structural evaluation of the residual load carrying capacity, destructive and non-destructive testing was performed along with petrographic examination of the concrete core samples to determine heat profiles throughout the reinforced concrete bridge deck and within the prestressed concrete girders. Prestressing strands, mild reinforcing steel, steel drainpipe, and concrete cores were all extracted from the fire damaged zones for laboratory testing. Material strengths were adjusted for heat profiles determined from the petrographic examination and were then used for structural evaluation of the residual capacity for the bridge in its damaged state. Load testing results were used to validate a 3D Finite Element Model of the bridge to accurately determine structural demands. The structural evaluation and load testing determined that the bridge has sufficient residual capacity in its damaged state for unrestricted truck traffic as per the Canadian Highway Bridge Design Code (CHBDC), CSA S6-19, and the bridge was re-opened to full legal truck traffic 24 days following the incident in a single lane alternating traffic configuration.

This paper highlights key lessons learned from this project with respect to responding to a major fire incident and assessing heat damaged structures in terms of what to triage and prioritize in the response.

Figure 1. Sikanni Chief River Bridge

Source: WSP Canada Inc.

Emergency Response

The Sikanni Chief River Bridge is located at km 256.1 on the Alaska Highway (British Columbia Highway 97), between Fort St. John (South) and Fort Nelson (North) in Northern British Columbia. The structure is a five-span prestressed precast concrete channel girder bridge with five girder lines. The bridge structure is dated 1968. The bridge carries the two-lane Alaska Highway through a deep valley over the Sikanni Chief River. The bridge is situated on a constant grade of 3.5% and located close to the sag of a vertical curve in the highway alignment.

On August 25th, 2022, a transport tanker travelling north and carrying Condensate, Sweet – PG II, a flammable liquid, crashed into the southeastern approach barrier and caught on fire. The PG II flammable liquid spilled from the tanker onto the bridge deck and ignited causing a large fire on the bridge. The fire started on the top surface of the bridge deck, and then propagated to the underside of the deck via the deck drains, causing significant fire damage to the deck, concrete girders and diaphragms. WSP was engaged by PSPC following the accident to assess the damage and guide safe reopening of the bridge to traffic.

On the morning of August 26th, 2022, a bridge engineer flew to the Sikanni Chief River Bridge site to complete an emergency reconnaissance of the accident and provide a rapid damage assessment. When arriving at the bridge, the site was still under police control as the accident was still being investigated. Permission from the police was given to the bridge engineer to begin a rapid assessment of the bridge. During the police investigation the bridge was fully closed to all traffic and the public.

Figure 2. Spans 1, 2, and 3 of the Sikanni Chief River Bridge

Source: WSP Canada Inc.

When the bridge engineer arrived at the bridge site, the flames were extinguished but the scene was still hot. A rapid damage assessment through visual inspection was completed followed by interviewing the person that fought the fire. Visual inspection was completed from the bridge deck and from the ground level below the bridge. Significant spalled areas of concrete were observed on the underside of the girders on Span 1 and Span 2 along with localized areas of spalled concrete on the underside of girders within Span 3. Within Span 1 and Span 2, the damage was most severe on the exterior girders near the drain outlets.

The bridge deck showed signs of fire damage on the parapets with exposed aggregate and localized spalling on the traffic face of the concrete barriers on the south end of the bridge. When interviewing the individual that fought the fire, the responding bridge engineer learned that a tandem axle water truck was used for fire suppression and was driven down the centre portion of the bridge. The water truck was filled five times (at the north approach to the bridge) and travelled the full length of the bridge to fight the fire at the south approach. This resulted in 10 passes of the truck over the entire length of the bridge, 5 passes with the truck full of water, and 5 passes with the truck empty. The water truck vehicle registration was reviewed, and the net vehicle weight was listed as 19,700 kg with an operating gross vehicle weight (GVW) of 29,550 kg.

Considering that the bridge was able to carry a fully loaded water truck over its entire length for 5 passages during the initial response to the fire and several heavily damaged areas were located on the exterior girders, it was determined that the bridge could be re-opened to single rear axle passenger vehicles in a single lane alternating configuration down the centre of the bridge. Based on this recommendation, the bridge was re-opened under these restrictions immediately, once the police released the site back to PSPC on the evening of August 26th, 2022.

Forensic Review

Within hours of the accident, a forensic review of the structure to determine the extents of the damage was initiated and continued for 24 days. This included destructive and non-destructive testing, with a special emphasis on petrographic examinations to determine the temperature profile through the concrete members. Concurrently, a thorough literature review was undertaken to develop an understanding of the impact of the highly elevated temperatures on the material properties, and to inform the structural evaluation undertaken.

<u>Non-destructive Testing</u>

Visual Structural Inspection

A visual structural inspection was undertaken from a snooper truck on August 27th, 2022. The inspection focused primarily on the fire damaged spans (Span 1 and Span 2 at the south end). Moderate to severe concrete spalling was observed on the underside of girders, with some exposed strands and stirrups in the worst case. However, concrete was generally sound when hit with a handheld hammer. Other bridge elements including barriers, bridge deck, soffit, bearings, Pier 1, Pier 2, and the South Abutment were also visually inspected. Localized damage was noted in a few locations; however, concrete was generally found to be sound on all elements. It is noted that visual heat mapping based on concrete colour was not completed. The bridge was covered in soot, which may have deposited during the later, less intense stages of the fire event hence potentially masking high heat zones. The evaluation Team ultimately decided not to formalize any visual heat mapping for the concern of reporting inaccurate results.

Bridge Deck & Parapet Delamination Mapping

Following the visual structural inspection, a partial chain drag test was performed on the bridge deck on August 29th, 2022, to identify locations of concrete delamination. Additionally, partial hammer sounding of the east parapet was also performed to locate concrete spalls. Bearing assemblies were inspected at the south and north abutments. No major damage was found due to fire damage. The exposed surfaces of the parapet wall had light scaling to medium spalling with exposed aggregates, due to fire damage on the exposed (traffic) sides of the barriers.

Surveying
A baseline survey was completed on September 4th, 2022, and two monitoring surveys were subsequently completed on September 9th and October 6th, 2022. All surveys were completed using a conventional total station and prism.

A total of 150 points were surveyed including 18 punch marks located at the expansion joints and 132 drilled holes along the bridge deck. The trend of all 150 points surveyed on the bridge showed little to no movement.

Girder Damage Mapping
To better visualize and further understand the condition of the superstructure, visible damage on the girders was mapped out on September 8th, 2022. Since a conventional rating system such as the one used in the Bridge Inspection Manual (BIM) would have assigned an Urgent rating to all damaged areas, a more focused rating system was employed to categorize three (3) severity levels for visible fire damage as follows:

- Light scaling and spalls up to 10 mm in depth were categorized as light damage.
- Spalls ranging in depths from 11 mm to 30 mm were categorized as moderate damage.
- Spalls exceeding 31 mm in depth were categorized as severe damage.

The locations with severe damage, and exposed rebar and prestressing strands, were concentrated primarily within the bottom flanges and underside of the girders.

Schmidt Hammering
Hardness testing was undertaken on September 9th, 2022, using a Schmidt hammer, testing girder flanges and webs, and pier hammerheads.

Testing was performed at varying web locations and along various stations on the girders and pier hammerheads. For cores, test values were taken at surrounding areas where samples were extracted. Testing locations were selected based on accessibility and representativeness of the various bridge elements. In accordance with *ASTM C805/C805M-18*, a minimum of 75 readings per representative type of element and a minimum of 20 readings per core location were performed.

The purpose of the tests was to determine the relative changes in concrete hardness along the length of each element and determine whether there is any correlation between fire damage and hardness values. In general, rebound readings were lower in the fire damaged regions, which can be an indication of a lower compressive strength for concrete in fire damaged zones compared to the undamaged regions. It should be noted that the hammering results are more representative of the quality and compressive strength of the surface concrete rather than the in-depth concrete.

Monitoring Structural Inspections
Following the initial response, visual inspections were completed daily from August 27th to September 21st, 2022, to ensure that any significant changes would be detected as soon as possible. The visual inspection included a topside walk of the bridge deck and approaches, and underside inspection from the ground level at both ends. Damaged components near the south abutment were inspected up close where accessible from underneath. No observable changes were identified during this period.

Petrographic Examinations

The purpose of the petrographic examination was to identify damage features specifically associated with concrete exposure to fire and elevated temperature and to estimate a temperature profile through the cross section of a fire damaged member to determine residual capacity. Information such as mix design, concrete specification, and construction procedures/methods for the construction of the Sikanni Chief River Bridge were not available for review. As such, the effects of exposure to fire and elevated temperatures, along with the general quality of the concrete from a materials engineering perspective was determined from results and observations obtained during petrographic laboratory examination of the samples provided (Table 1).

Table 1. Cores for Petrographic Analysis

Bridge Component	Core Location	Core Label	Concrete Condition
Web – East Leg	Girder 5 Span 1 Web East Leg	G5S1WE2	Exposed to fire and elevated temperatures
	Girder 5 Span 1 Web East Leg	G5S1WE4	Exposed to fire and elevated temperatures
Diaphragm	Girder 4 Span 5 Diaphragm 1	GN4C	Unaffected area
	Girder 1 Span 1 Diaphragm 3	G1S1D3	Exposed to fire and elevated temperatures
	Girder 3 Span 1 Diaphragm 3	G3S1D3	Exposed to fire and elevated temperatures
	Girder 5 Span 1 Diaphragm 3	G5S1D3	Exposed to fire and elevated temperatures
Deck Overlay	Deck – north span	DN1	Unaffected area
	Deck – south span	DS2	Exposed to fire and elevated temperatures
	Deck – south span	DS5	Exposed to fire and elevated temperatures

Two cores (GN4C, DN1) were used as control specimens to represent the service condition of the girders and deck respectively. Figure shows an example of the heat profiles, detailed for two of the concrete deck cores and one of the diaphragm cores.

Figure 3. Heat profile for deck cores DS2 (left), DS5 (centre) and G1S1D3 (right)

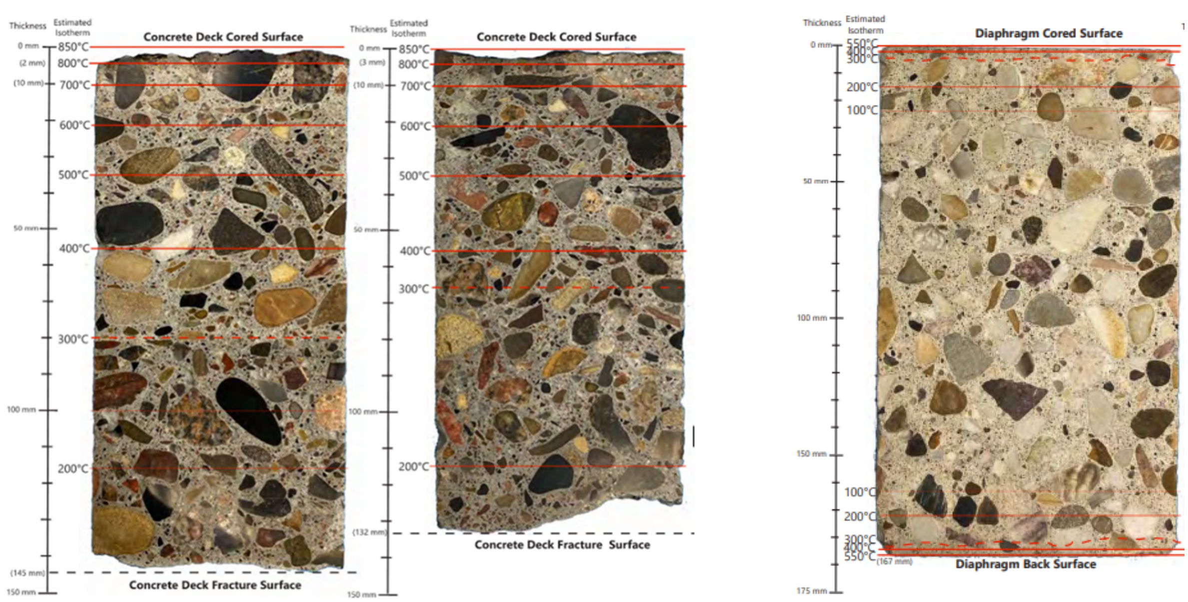

Source: WSP Canada Inc.

The concrete core specimens were cut parallel to the long axis, exposing a cross-sectional surface that was polished to a high finish suitable for petrographic examination based on *ASTM C856-20*. Thin section specimens of the cross-sectional surface of companion portions of each core were also prepared to provide detailed insight into the overall quality of the cementitious paste and microfeatures commonly associated with fire and heat distressed concrete. Polished cores and thin sections were delivered to a laboratory for petrographic examination.

Some of the attributes used to determine the profile of heat experienced through the depth of the concrete cores include:

- Dark grey coloured, anisotropic, cementitious paste displaying intense cracking that indicated the cores removed from the webs and diaphragms were exposed to a surface temperature that exceeded 300°C.
- Gradational pink colouration due to oxidation of FeOH (iron hydroxide) within the cementitious paste and some arenite and other siliceous aggregate particles was observed to depths that were up to 15 mm from the cored surfaces (along pre-existing cracks). This reddish discolouration and the decrease in the intensity of interconnected sub-parallel and perpendicular micro-cracks (boundary and intrapaste) within the cementitious matrix and within quartz grains indicated the extent of 300°C temperatures approximately 10 mm to 15 mm from the cored surface and 5 mm to 10 mm from the back surfaces.
- Discolouration of the cementitious paste within deck cores were observed as a charred, dark grey colour up to 5 mm overlying a light buff colour up to 20 mm.
- Underlying the light buff cementitious paste was a light grey colouration to a depth of 80 mm associated with random dark red/pink coloured patchy areas within some siliceous aggregate, indicating the 300°C isotherm.

Features associated with temperature exposure lower than 300°C could not be discerned based on thin section microscopy. Temperature profiles were based on petrographic observations denoting the 300°C isotherm and extrapolated from experimental temperature curves recorded on a 200 mm concrete rib exposed to heat from three sides (web and diaphragm) and experimental temperature curves recorded on standard blast furnace tests of slab exposed to heat from single surface (deck).

These results presented in Table 2 were used to inform the evaluation of the damaged structure.

Table 2. Estimated Temperature Profile by Bridge Component

Location	Estimated Temperature (°C)	Depth
Girder Web – East Leg	550	up to 3mm below cored, finished surface
	300	10 to 12 mm below the cored, finished surface
	100	35 mm to 40 mm below the cored, finished surface
	100	25 mm to 30 mm below the back, finished surface
Diaphragm	550	up to 0.5 mm below the cored, finished surface
	300	4 to 15 mm below the cored, finished surface
	100	20 mm to 25 mm below the cored, finished surface
	100	20 mm to 25 mm below the back, finished surface
Deck	850	surface temperature
	300	65 to 80 mm below the cored, finished surface
	200	120 mm below the scaled surface

Effect of Extreme Heat on Material Properties

An accurate temperature profile through the concrete members impacted by heat damage provides important information for the strength evaluation of the structure. Two methods are commonly used to determine the material temperature that is experienced during a fire:

- Petrographic Examination
- Fire Simulation Modeling

Temperature is especially important for concrete members since:

- Damage to concrete due to extreme heat is expected to be permanent.
- Due to the large through-thickness temperature gradients in concrete members, heat profiles and associated concrete effects will differ by internal locations.

In the case of the Sikanni Bridge Fire response, direct evaluation of prestress loss due to heat damage was very difficult which resulted in material strength and prestress loss being estimated using the temperatures determined through petrographic examination.

Fire simulation requires good qualification of the fire source, location, size, duration, and further information that was not available with certainty for the Sikanni Chief River Bridge. Fire simulation is also limited in its relevance as most fires are non-standard. As a result, petrographic analysis was completed as the means for determining the temperature profile through concrete cores extracted from both control locations without fire damage and relevant locations of fire damaged members.

Concrete Residual Strength

Significant research regarding concrete strength exposed to extreme temperatures has been completed by others and shows that large reductions in concrete strength can occur. The dissertation by W.L. Moore compiled the results from a large number of previously completed research data on fire damaged concrete and came up with a best-fit curve to estimate the fire damaged compressive strength of concrete. The results of this best fit curve are shown in Figure .

Figure 4. Residual compressive strength of concrete vs. temperature

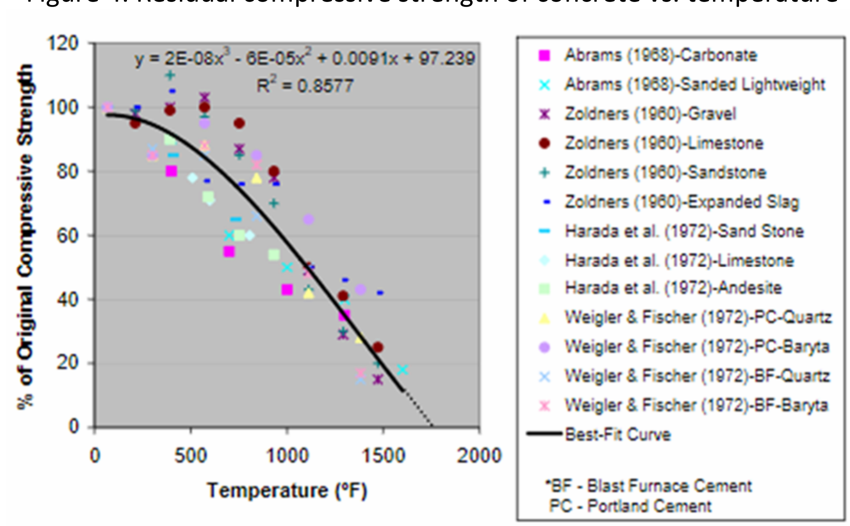

Source: Moore, 2008

We used this best-fit curve in conjunction with the petrographic results to determine the concrete strength reductions at different internal temperature intervals for the deck and girders.

Mild Steel Residual Strength

Mild-reinforcing steel acts in a similar way to structural steel when exposed to extreme temperatures. Typically, there is only significant permanent reduction in rebar strength at the most extreme temperatures. Based on the petrographic results the reinforcing for Sikanni Chief River Bridge did not experience temperatures over 300 degrees Celsius. We used the graph in Figure for residual reinforcement strength which is based on the research paper by W.P.S. Dias to determine the yield strength reduction used in the post-fire capacity calculations.

Figure 5. Residual strength vs. temperature for mild-reinforcing steel

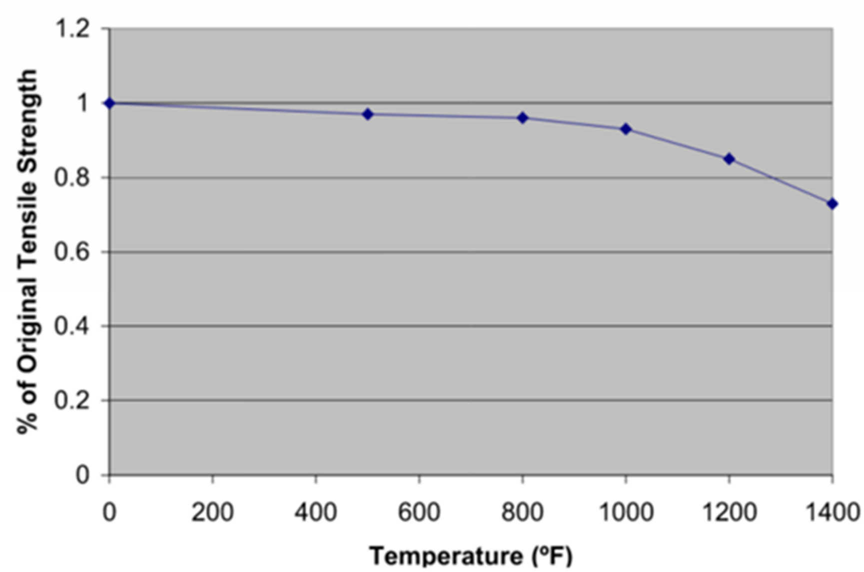

Source: Dias, 1992

Prestressing Residual Strength

High strength prestressing strands are sensitive to extreme temperatures and can experience large reductions in material strengths. To determine the residual tensile strength of the prestressing strands exposed to fire in the Sikanni Chief River Bridge, the model proposed in the thesis by Kevin Maclean was used. The equation for this model is shown below where T is the temperature the strand was exposed to:

$$f_u(T) = 0.25 + \frac{0.75}{1 + (\frac{T}{550})^{6.5}}$$

Residual Prestressing Force

The amount of prestressing force in the girder strands can be affected by extreme temperatures due to thermal expansion and creep. Experiment test data completed by Kevin Maclean shows that minimal and gradual prestress loss occurs for temperature up to 300 degrees Celsius. After 300 degrees Celsius the rate of prestress loss becomes much greater. The residual prestress ratio corresponding to Figure was used in the post-fire girder capacity calculations.

Figure 6. Experimental prestress loss

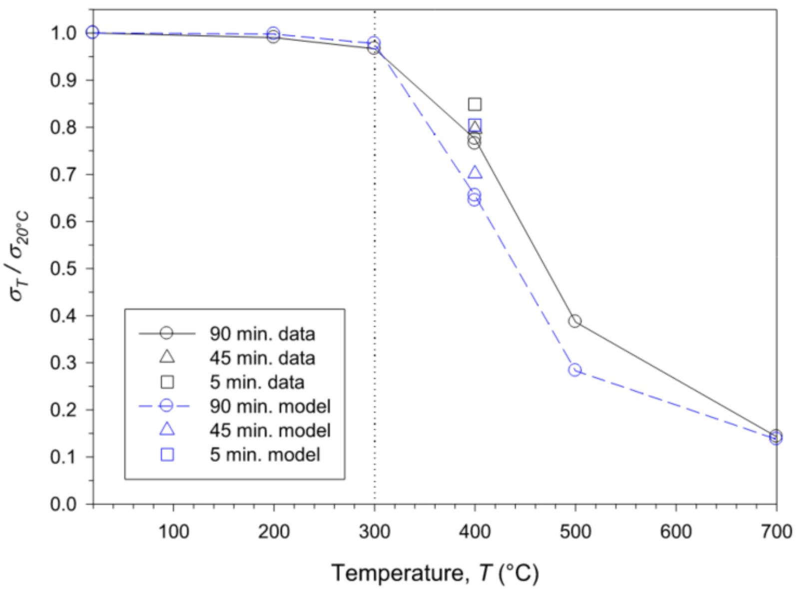

Source: MacLean, 2007

Residual Bond Strength

Research has shown that the bond strength between the prestressing strands and surrounding concrete will reduce when exposed to extreme temperatures. However, little research has been done to estimate this reduction with varying temperatures and concrete strength. With a reduced bond stress, the prestressing strand development length increases. This in turn reduces the moment and shear capacity near the end of the girder spans, as the effective area of a strand is reduced within the increased development length. We did not modify the development length due to:

- Petrographic analysis results indicating that the strands were not exposed to a temperature greater than 300 degrees Celsius.
- The majority of the damaged girder zones which would have experienced the highest temperatures are located beyond the 2.3m strand development at each end of the girders indicating an even lower temperature than 300 degrees Celsius at these locations.
- Strands were omitted from the capacity calculations when strands were exposed and consequentially the bond stress was reduced within the development length.

Destructive Testing

Concrete Core Testing

61 concrete cores of approximately 69 mm (3”) and 100 mm (4”) in diameter were collected from the main structural elements and visually examined. Of these, a sample size of 17 and 9 cores were selected for compressive strength and petrographic examination, respectively. Remaining cores were preserved for future testing, if required. Cores were collected at representative areas of both damaged and undamaged locations of the bridge to allow for comparison. As such, all cores were either extracted from high heat zones (i.e. Span 1) or no heat zones (i.e. Span 5).

Figure 7. Span 1 core locations

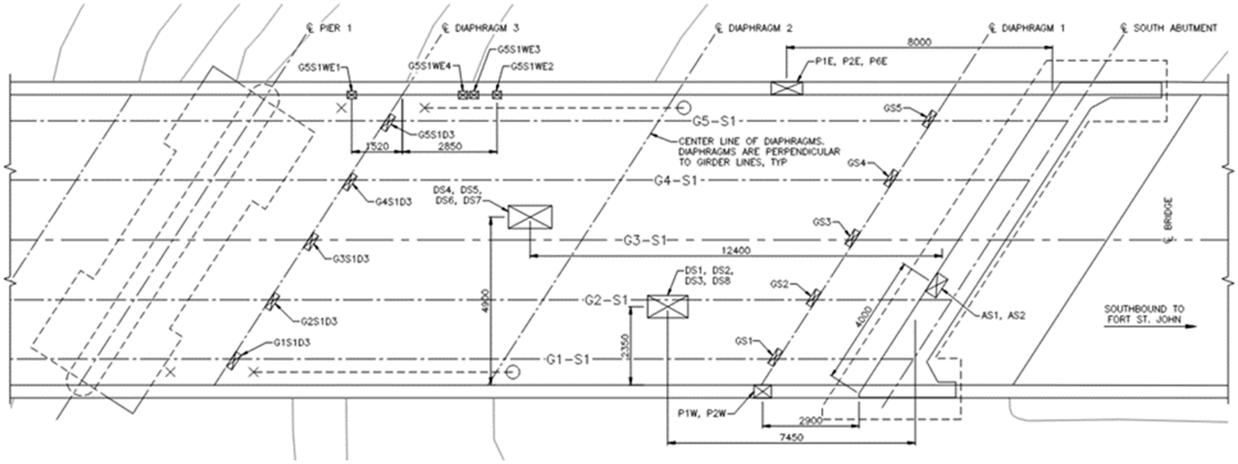

LEGEND			
CORES	**LOCATIONS**	**CORES**	**LOCATIONS**
G5S1WE1 — GSS1WE4	GIRDER 5 SPAN 1 WEB — EAST LEG	**AS1 — AS2**	ABUTMENT — SOUTH SIDE
G1S1D3 — G5S1D5	GIRDER 1—5 SPAN 1 DIAPHRAGM 3	**P1W — P4W**	PARAPET — WEST SIDE
GS1 — GS5	GIRDER 1—5 SPAN 1 DIAPHRAGM 1	**PR1N1 — PR1N2**	PIER 1 — NORTH SIDE
DS1 — DS8	DECK — SOUTH SIDE	**PR1S1 — PR1S2**	PIER 1 — SOUTH SIDE
P1E — P6E	PARAPET — EAST SIDE		

Source: WSP Canada Inc.

Compressive strength tests were conducted in accordance with *CSA A23.2-14C* with the petrographic examination conducted in accordance with *ASTM C856/856M-20.*

Steel Drainpipe Mechanical Testing

A sample of approximately 406 mm long steel drainpipe at the northwest corner of Span 5 was tested to provide baseline properties of drainpipe not affected by fire. Two additional samples of approximately the same length, taken at the southeast and southwest corner of Span 1 (high heat zone), were subsequently tested. The purpose for collecting samples of the steel drainpipe was to allow for comparative review of impacts to mild steel within heat impacted zones compared to non-heat zones. Since the steel drainpipes were relatively easy to access, they were included in the testing program to contribute to the understanding of heat impacts to the structure.

Drainpipe mechanical testing was conducted in accordance with *ASTM A370-21*. The results showed that the overall heat did not significantly impact the mechanical properties of the steel drainpipes.

Prestressed Strands Testing

Mechanical and microhardness tests were performed on four prestressed strand samples. Two strands were extracted directly from the high heat zones, while two strands were extracted from minimal heat zones to allow for results comparison. The strand lengths before and after cutting were measured to calculate strand shortening and estimate tension forces. Mechanical testing was conducted in accordance with *ASTM A1061/1061M-20a*. Microhardness testing was conducted in accordance with *ASTM E92-17*. Material properties and hardness readings were compared to evaluate the effects of heat and residual strength of strands.

Reinforced Steel Testing
Two 10M reinforcing steel samples of 254 mm and 406 mm in length were removed from Span 1 Girder 2 East Leg. The shorter bar was in the concrete spalling region (high heat zone), while the longer bar was taken from fully embedded concrete (low heat zone). Mechanical testing on reinforcing bars were performed in accordance with *CSA G30.18:21*.

Load Testing
To understand how the fire damage could impact the structural response of the bridge, the evaluation Team installed instrumentation and performed load testing. A comparative testing approach was taken whereby the response of Span 5 (undamaged) was compared to the response of the Span 1 (fire damaged) under similar loading conditions. This approach had several benefits including rapid mobilization/installation and efficient data analysis. Since the span configurations were identical and the sensors were installed in a symmetric manner, any differences in response could be quickly identified and quantified. The results of the load testing were early indicators of bridge performance on both a global and localized scale, were used to refine the load evaluation, and ultimately validated the findings from the material testing.

Instrumentation
The structural monitoring system was designed to be rapidly deployed, installed, and removed. The following instrumentation was installed in a symmetric manner (see Figure):

- Strain Transducers – 13 strain transducers were installed near midspan of each of span (26 total). These sensors provided insight into the localized behaviour of each span (i.e. lateral load distribution, load magnitude, location of neutral axis, etc.);
- Displacement Gauges – one displacement gauge was installed at midspan of the approach spans (2 total) along centreline of the bridge. These sensors provided insight into the global behaviour of each span; and
- Rotation Tiltmeters – three tiltmeters were installed on the underside of girder webs at each abutment (6 total). These sensors provided insight into the global behaviour of the bridge, easily identifying whether the spans were behaving in a linear elastic manner.

Figure 8. Overview of instrumentation

Source: WSP Canada Inc.

Diagnostic Testing

The approach to load testing included two types of diagnostic testing: a semi-static moving load test and a static load test. For the moving load test, only vehicles with a precedent of already crossing the structure were used (the snooper truck and the water truck, 21 tonnes and 30 tonnes respectively). The trucks were positioned in three transverse locations and were driven across the structure (in both directions) at a speed of ~ 5 km/hr. Two tests were completed for each truck in each position. In addition to knowing the transverse location of the trucks, the axle locations were tracked so that the longitudinal truck position could be known within +/- 150 mm. The sensors were zeroed before each test to maximize data clarity and data were collected at 50 Hz.

Figure 9. Moving truck loads

Source: WSP Canada Inc.

For the static load test, 17 precast concrete barricades were precisely placed at midspan of each span along with a skid steer. The objective behind the static load test was to provide insight into how the in-situ deflection of the structure compared with the theoretical deflection from the finite element model.

Figure 10. Static load test

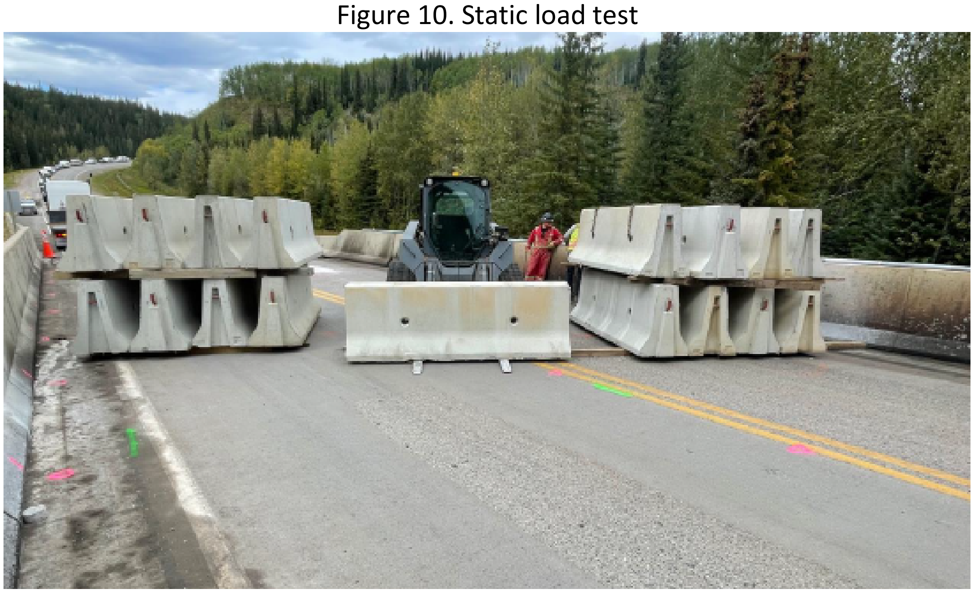

Source: WSP Canada Inc.

All field data was examined graphically to provide a qualitative assessment of the structure's live load response and data quality. In general, the response data was found be of good quality and typical magnitudes/shapes for prestressed girder bridges.

Figure 2. Example of data quality

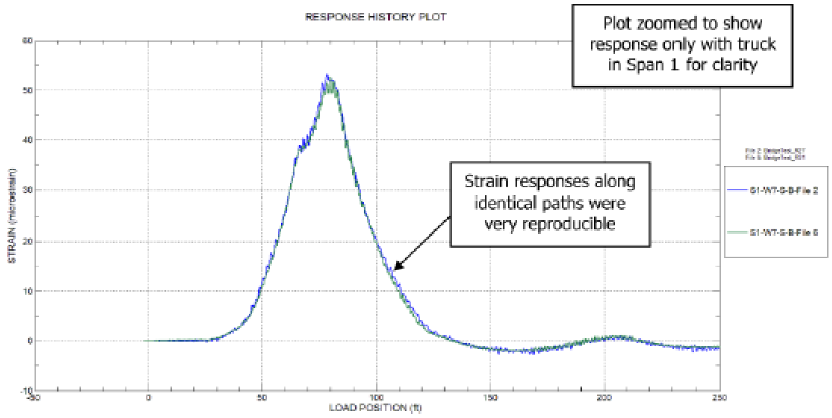

Source: WSP Canada Inc.

Load Testing Results

The results from the load testing provided valuable information at an early stage in the structural evaluation. They ultimately contributed to the unrestricted re-opening of the structure and are summarized as follows:

- The comparative analysis revealed that the damaged span was performing linear elastically and in a similar manner to the undamaged span. In general, the global response magnitudes measured in Span 1 matched reasonably well with the undamaged Span 5 response. On a localized level, strain magnitudes varied on a few of the girder webs. The more damaged locations were showing incrementally smaller strain than their undamaged equivalent. While the differences were small in magnitude, this phenomenon isn't atypical for a bridge that has sustained some degree of damage (i.e. reduced section/stiffness, microcracking, etc.) as load tends to be shed both transversely and longitudinally away from the damage.
- The load testing results contributed to the refinement of the computer model (ie, by calibrating for stiffness of components such as reinforced concrete barriers) and to the reduction in uncertainty in structural evaluation, resulting in an overall improvement to the live load capacity rating of 40%.
- The positive results from the load testing supported the localized material testing results and showed that it was reasonable to extrapolate these results to a global level.

Figure 3. Example of response symmetry between spans

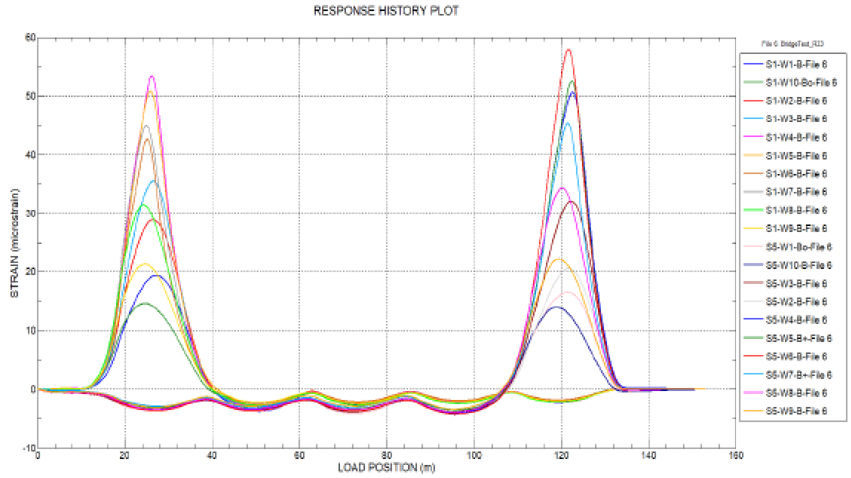

Source: WSP Canada Inc.

Phase 2 Load Testing

A second round of load testing was completed several months after the fire incident to ensure that strengthening of the structure was not required to meet the full CSA S6-19 design load. A similar, but more robust approach to instrumentation was taken during this round of testing, building upon lessons learned from the first round, and expanding the instrumentation to include Span 2. To emulate a CL-625 design load, a local company loaded a truck at the evaluation Teams direction such that the load effects very closely matched the theoretical CL-625 design vehicle. Both static moving load tests (<5 km/hr) and dynamic moving load tests (50 km/hr) were completed to provide insight into the dynamic load effect.

Figure 4. Equivalent CL-625 test truck

Source: WSP Canada Inc.

To ensure that the bridge did not become overloaded during the load test, stop criteria were established. The first criterion was a maximum allowable strain measurement (>270 microstrain) based upon the theoretical response of two unfactored CL-625 design trucks. The second criterion was the observation of inelastic behaviour from any sensor.

Figure 5. Load effect comparison

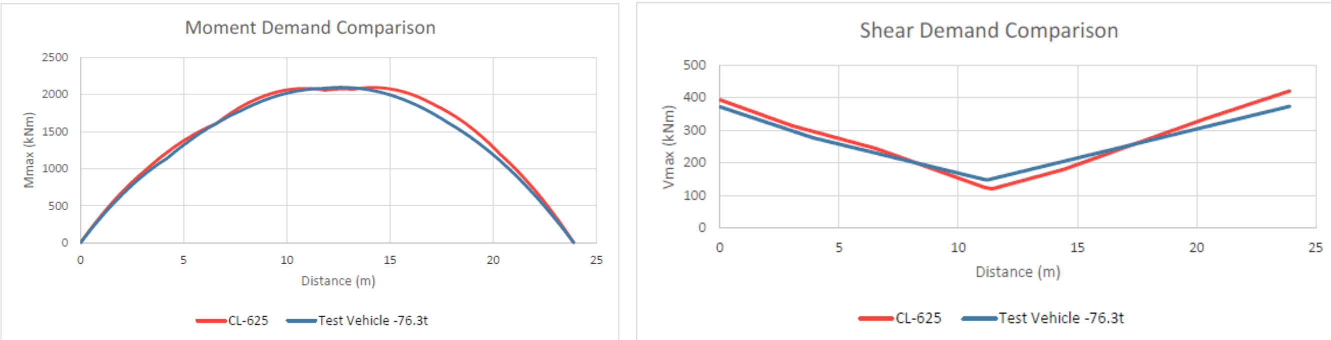

Source: WSP Canada Inc.

The findings from the Phase 2 Load Testing were:

- The structure responded linearly elastically under all tested conditions;
- The dynamic load amplification depended on the direction the truck was travelling and varied between the spans, ranging from 1.03 to 1.09;
- The results were within the elastic range of the prestressed concrete and much less than the pre-determined stop criteria;
- The analytical model conservatively predicted the structural response (i.e. all in-situ responses were less than predicted by finite element model); and
- Span 1 and 2 (damaged) performed in a comparable manner to Span 5 (undamaged).

The above findings demonstrated that the fire did not cause an appreciable loss of structural capacity up to the CL-625 design load and that strengthening of the girders was not required.

Structural Evaluation for Load Rating

3D Finite Element Model

Sikanni Chief River Bridge consists of multi-simply supported spans with nearly identical span lengths. A 3D finite element grillage model was developed using CSiBridge as shown in **Error! Reference source not found.**, for a typical span length of 24.6 m, to determine the live and dead load demands per girder. The model was built for the superstructure only. As-built drawings indicates that reinforcing steel projects from the girder webs into the concrete deck overlay, providing composite action between the girder and deck overlay. Therefore, a composite section consisting of the girder and deck overlay was used in the model analysis.

Figure 6. 3D grillage model used for Sikanni Chief River Bridge load capacity evaluation

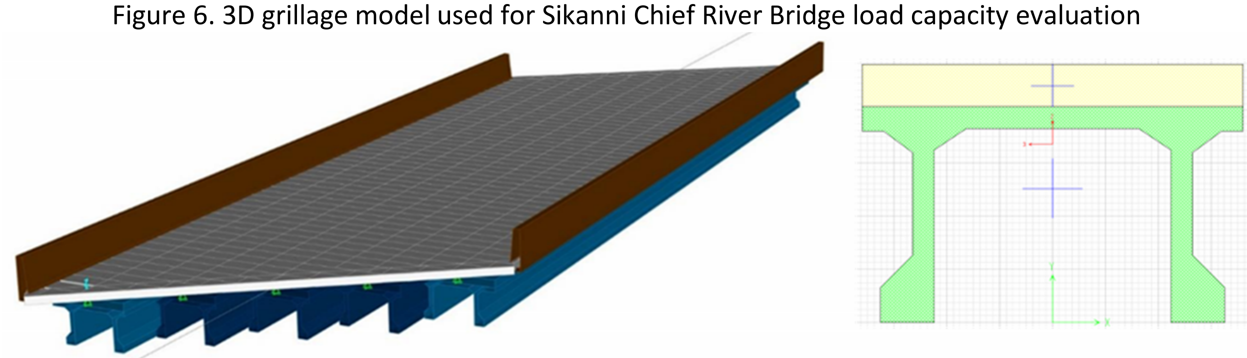

Source: WSP Canada Inc.

The bridge was evaluated for a CL1-625 design vehicle under normal traffic loading. Live loads, dead loads, and load factors were all included in accordance with Section 14 of CHBDC, CSA S6-19.

The data from the load testing was used to calibrate the refined computer model to determine load effects. In particular, the static load test was replicated in the model and compared to the in-situ response. It was found that the model was behaving very similarly with a deflection being within 10% of the actual measured response. This indicated that the model was able to capture realistic responses to the applied loading and that further calibration was not required.

Influence of Petrographic Examination on Member Capacities

Since the strength of materials can be significantly reduced by exposure to extreme heat, petrographic examination was completed to accurately determine the temperature profile through the deck and girder concrete. The internal temperature of concrete was essential to allow for assessments of the material properties based on start-of-art research on post-fire material properties. The material properties were modified based on the results of the petrographic examination and are shown in Table 3 and Table 4.

Table 3. Modified Material Properties for Analysis

Material Property	Petrographic Temperature Results (°C)	Residual Strength (%)
Concrete Residual Strength	Varies with depth – see next table	
Mild Steel Residual Strength	<300	96
Prestressing Steel Residual Strength	300	98.6
Residual Prestressing Force	300	96
Residual Bond Strength	300	100

Table 4. Modified Concrete Compressive Strength for Analyis

Girder Web Depth (mm)	Petrographic Temperature Results (°C)	Residual Compressive Strength (%)
0 (girder surface)	550	56
10	300	83
51 (girder centerline)	0	100
Deck Depth, from top surface (mm)		
0 (riding surface)	850	15
5	850	15
20	600	48
80	300	83
200	0	100

Live Load Capacity

Based on the detailed structural evaluation, it was determined that the Sikanni Chief River Bridge had adequate structural capacity in its damaged state to support unrestricted truck traffic in accordance with CHBDC, CSA S9-19. While the bridge suffered from a loss of capacity in its damaged state, the remaining capacity was adequate to support unrestricted truck traffic.

Long Term Durability

The permanent structural damages, if not repaired, would have had significant impact on the long-term durability, hence, remaining service life of the bridge. The most significant structural damage was concentrated on the underside of the bridge due to the spalled concrete that had exposed prestressing strands and reinforcing steel. There was also loss of durability on the bridge deck and barriers.

Contingency Plans

From the time the accident occurred, we assembled many teams working concurrently to ensure the bridge could safely reopen to traffic as quickly as possible. These teams had to shift their focuses as the work progressed and more data became available. Initially, there was an urgency to confirm a detour crossing, including re-activating decommissioned alignments and installing temporary structures. However, it was quickly determined that rapid implementation of a detour crossing would not be feasible. This led to a further exploration of installing a temporary modular structure on top of the damaged span of the Sikanni Chief River bridge, but this was ultimately determined to be an impractical solution.

Two different strengthening design options were advanced to sealed tender ready packages including drawings and specifications, though ultimately neither was necessary as the bridge was confirmed to have adequate residual structural capacity in its damaged state.

Strong Back Strengthening

Had the shear and moment capacity been found to be insufficient, a “strong back” strengthening option was developed to safely restore single lane alternating full legal load traffic to the structure. This design consisted of using steel plate girders, which PSPC already owned and had stored near the bridge site, on the deck with hanger supports provided under the bridge. Due to this distributing most of the load to the outside of the pier caps, additional bracing at the piers was also designed.

Fibre Reinforced Polymer (FRP) Strengthening

Had the shear capacity of the girders at the pier been found to be insufficient, an FRP strengthening option was developed to safely restore both lanes of full legal load traffic to the structure. This required the design of some concrete repairs and surface preparation, followed by the application of FRP wrap to approximately five meters of girders at the piers in the damaged spans.

Rehabilitation Design

After completing the load rating that determined the structure had adequate capacity for unrestricted loading in its damaged state, a rehabilitation design was undertaken to improve durability of the bridge. The rehabilitation design included a combination of concrete patches in locations with moderate to severe delamination and application of a sealer in locations of light scaling. The rehabilitation design also included reinstatement, and local re-tensioning, of the prestressing strands that were extracted as part of the destructive testing program.

Concrete patch repairs on the piers and abutments included epoxied dowels and welded wire mesh while the patch repairs on the bottom flange of the girders included stainless steel pins to strengthen the bond of the patch material to the girders. While reviewing repair alternatives, consideration was given to using fibre reinforced polymer (FRP) wrapping of the damaged girders after the concrete patching was complete; however, this was not carried forward as the FRP wrapping was not required for strengthening and the cost of using FRP for improving durability was not justified.

Lessons Learned

An effective and timely response to a fire damaged bridge requires a strong team and a detailed knowledge of how heat profiles within the structure can negatively influence material properties resulting in a decrease of structural capacity. Some specific lessons learned from our experience responding to the Sikanni Chief River Bridge fire are summarised below.

Importance of Prioritizing Petrographic Examination

An obvious priority following fire damage to a bridge is to get an experienced bridge engineer to site as quickly as possible to offer a rapid damage assessment. An exceptional on-site rapid response was provided at Sikanni that included several highly qualified bridge engineers. If a future incident occurs, we will also prioritize getting a petrographic examiner to site to join the bridge engineers. While the bridge engineers can identify locations for concrete core extraction for the petrographic examination, having the petrographer come to site to review the heat damage firsthand will enable a clearer view of the structure and associated heat damage and will assist by accelerating the laboratory petrotraphic review period. Since time can be lost due to shipping of the cores, having the petrographer on-site also enables them to return to their laboratory with samples “in hand” to further accelerate the timelines for the petrographic examination. In the case of our response at Sikanni, petrographic examination ended up being a critical path item even with incredible efforts that were made to accelerate each step of the process.

Discolouration of Concrete Resulting from Extreme Heat

For reinforced concrete, literature will provide references for various stages of discolouration that concrete will experience corresponding to specific temperature ranges. In our experience responding to the Sikanni Chief River Bridge, the fire damaged sections of the bridge were heavily covered in black soot, and it was not possible to use discolouration as a method for determining heat profiles. Since the petrographic examination determined that extreme heats were realized at Sikanni, we suspect that the black soot may have formed during the later stages of the fire in which temperatures were less severe. If discolouration of the concrete was visible, it may have assisted in identifying areas of focus for extraction of cores for our petrographic examination, but it would not have been relied upon as the sole source for determining the level of heat exposure for the bridge.

Reductions in Material Strengths Due to Heat Exposure

If sustained exposure to extreme heat has occurred, conventional material testing should be paired with petrographic examination to determine if reductions in material capacities should be applied in the structural evaluation and load rating. Temperatures exceeding 300 degrees Celsius are of particular concern. Petrographic examination is of critical importance for two reasons: it follows a recognized standard to reliably report temperatures; and it provides temperatures at critical depths corresponding to key structural elements such as prestressing strands and mild reinforcement. If the heat damage versus depth is not known there is a high risk of inaccurately over-estimating the loss of strength which may result in costly and unnecessary strengthening repairs.

Assign a Triage Lead and Mobilize a Strong Team

Consider assigning a senior bridge engineer as a Triage Lead; select someone who is experienced, practical, and performs well under pressure. Whenever possible, do not assign multiple responsibilities to the same person when tasks can be separated and distributed among a team of multiple professionals. For the Sikanni response, there were six separate and concurrent bridge engineering teams all working in parallel to get the bridge re-opened as quickly as possible while also providing tender ready contingency plans as part of the risk management strategy. During the initial response we found that daily meetings (including weekends) with the leads from both the consultant and the owner were beneficial to allow for synergies between concurrent efforts and to allow for open communication on all key developments.

Conclusion

In our response to the Sikanni Bridge fire, we found that the combination of petrographic examination and load testing were key to providing us with the information and confidence that was required to complete the necessary structural evaluations that enabled quick reopening of the bridge while avoiding unnecessary strengthening. Since the bridge was found to have adequate capacity in its damaged state, the strengthening designs that were completed as part of the larger risk mitigating strategy were not required; however, they provided a valuable contingency that would have enabled rapid implementation of strengthening repairs if the structural evaluation had found that the bridge did not have capacity for unrestricted traffic.

References

Dias, W.P.S. “Some properties of hardened cement paste and reinforcing bars upon cooling from elevated temperatures.” Fire Mater., 16: 29-35. (1992)

MacLean, K. J. “Post-Fire Assessment of Unbonded Post-Tensioned Concrete Slabs: Strand Deterioration and Prestress Loss.” Kingston ON: Kevin J.N. MacLean. (2007)

Moore, W. L. “Performance of Fire-Damaged Prestressed Concrete Bridges.” Missouri USA: Wendy L. Moore. (2008)

ASTM International C856-20. “Standard Practice for Petrographic Examination of Hardened Concrete.” West Conshohocken USA: ASTM International. (2020)

Canadian Standards Association (CSA) A23.2-14C. “Concrete materials and methods of concrete construction.” Toronto Canada: Canadian Standards Assosication. (2014)

ASTM International C856/C856M-20. “Standard Practice for Petrographic Examination of Hardened Concrete.” West Conshohocken USA: ASTM International (2020)

ASTM International A370-21. “Standard Test Methods and Definitions for Mechanical Testing of Steel Products.” West Conshohocken USA: ASTM International (2021)

ASTM International A1061/A1061M-20. “Standard Test Methods for Testing Multi-Wire Steel Prestressing Strand. ASTM International.” West Conshohocken USA: ASTM International (2020)

ASTM International E92-17. “Standard Test Method for Vickers Hardness of Metallic Materials.” West Conshohocken USA: ASTM International (2017)

Canadian Standards Association (CSA) G30.18:21. “Carbon Steel Bars for Concrete Reinforcement. Mississauga Canada.” Mississauga ON: Canadian Standards Association (2021)

ASTM International C805/C805M-18, A. “Standard Test Method for Rebound Number of Hardened Concrete.” West Conshohocken USA. ASTM International (2018)